INVESTIGATION OF SYSTEMS AND TECHNIQUES
FOR MULTICOMPONENT MICROFORCE MEASUREMENTS
ON WIND TUNNEL MODELS

Semiannual Status Report

on

NASA Grant NGR 47-005-026

Submitted by Co-Principal Investigators:

Dr. James W. Moore
Associate Professor of Mechanical Engineering

Dr. Eugene S. McVey
Associate Professor of Electrical Engineering

Research Laboratories for the Engineering Sciences

University of Virginia

Charlottesville

Report No. EME-4029-102-66U

March 1966

INVESTIGATION OF SYSTEMS AND TECHNIQUES
FOR MULTICOMPONENT MICROFORCE MEASUREMENTS
ON WIND TUNNEL MODELS

Semiannual Status Report

on

NASA Grant NGR 47-005-026

Submitted by Co-Principal Investigators:

Dr. James W. Moore
Associate Professor of Mechanical Engineering

Dr. Eugene S. McVey
Associate Professor of Electrical Engineering

RESEARCH LABORATORIES FOR THE ENGINEERING SCIENCES
SCHOOL OF ENGINEERING AND APPLIED SCIENCE
UNIVERSITY OF VIRGINIA
CHARLOTTESVILLE, VIRGINIA

Report No. EME-4029-102-66U
March 1966   Copy No. 4

TABLE OF CONTENTS

LIST OF ILLUSTRATIONS

FOREWORD

This is the six months progress report, covering the period of
15 July 1965 to 15 January 1966, on the development of a skin friction drag
sensor and also serves as a progress report on the multicomponent microforce
wind tunnel balance system. It is a continuation of work reported in University
of Virginia Report No. EME-4029-101-65U, dated August 1965. The remainder
of the research on the balance system will be published shortly in the form of
two theses, one on calibration and one on the electronic system.

SECTION I
INTRODUCTION

Major efforts have been made during the past semiannual reporting period on the measurement of skin friction and the measurement of multicomponent microforces. The multicomponent microforce measurement system is nearly completed and final data are being taken. It appears that all design objectives are either being met or can be achieved with minor modifications. It is anticipated that the breadboard system will be taken to Langley Field by the end of February. Two separate reports will be available by early spring; one on performance and calibration and the other on the electronics and control systems. One paper has been written and accepted for publication at the International Federation of Atomatic Control Conference to be held in June at London, England, and another is being written. One master's thesis has been written and theses are being written on this project.

The skin friction work involved the development and design of a laboratory model to serve as the basis for design of an operational prototype instrument, the development of high temperature components, and experiments on a pneumatic force measurement scheme. This report concerns primarily the skin friction meter work because as mentioned above, two other reports are to be published about the multicomponent system.

The following tentative specifications have been assumed for development purposes:

1) Force measurement range: The skin friction sensor is to be capable of measuring a force in the range of .7 to 7 millipounds

2) Temperature environment: The graph of figure 1 shows the variation of skin stagnation temperature versus time for a flight to mach 8 and 123,000 feet

3) Vibration: The sensor is to be capable of operating in environmental levels of 0.06-inch double amplitude at 10-55 cps and 10 g vibration from 55 cps to 2,000 cps

1
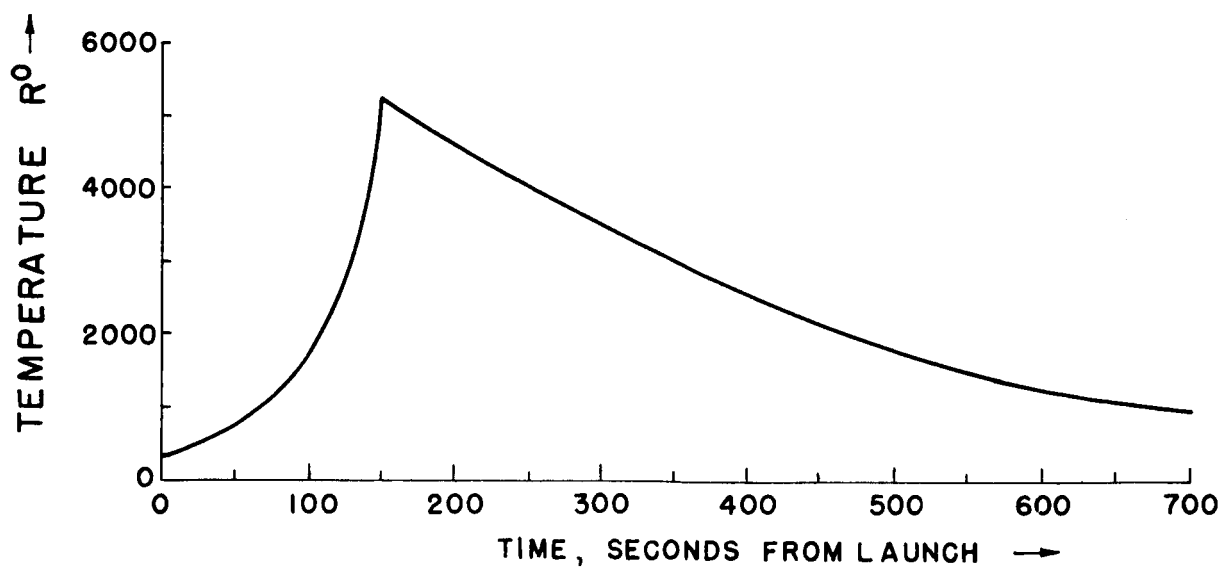
FIG. I SKIN STAGNATION TEMPERATURE VERSUS
TIME
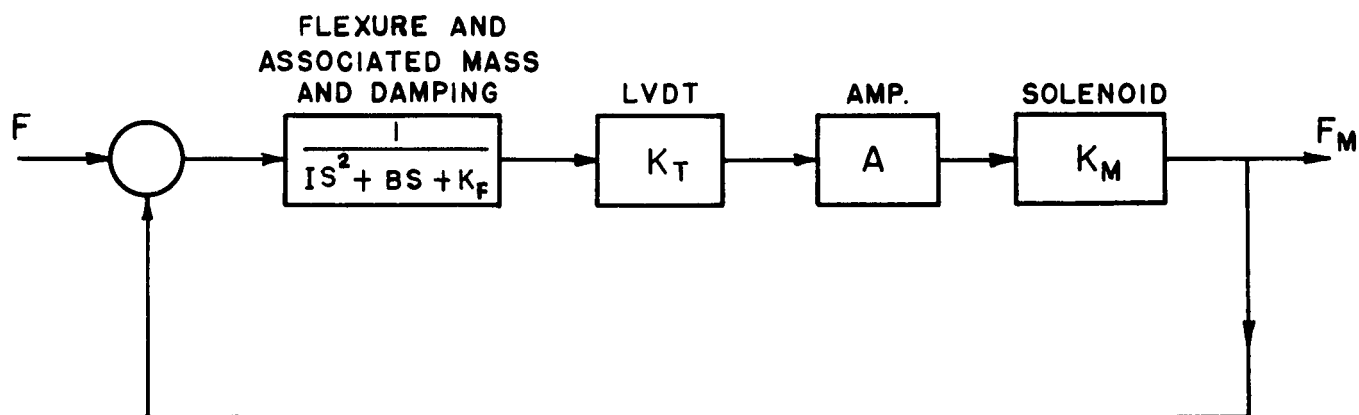
FIG. 2 BLOCK DIAGRAM OF CLOSE LOOP
SYSTEM

4) Acceleration: The maximum acceleration attained in the direction of flight is 3.5 g

5) Space requirements: The severest dimension restriction is the height (distance from skin to jet nozzle) which is 2". The other two dimensions can be somewhat larger

6) Available power: The power available on the X-15A-2 airplane is as follows:

a-c   3 phase 115 v (± 1 - 1 v) 400 cps (± 4 cps)

d-c   28 volts nominal; varies from 24-31 volts, ripple present at 2,400 Hz ± 0.5 v. Maximum of 10 amps available from each source.

SECTION II
A CLOSED LOOP EXPERIMENTAL MODEL

A laboratory model has been built to obtain verification of the theory for a closed loop type system and to explore the practicability of the general approach being adopted for operation in the hostile environment anticipated. Work by others [1, 2] has verified that a skin friction meter involving a small target of skin, flexures, displacement sensors and motors will work in a less hostile environment than the one being assumed for this work. Previous work done in the area and engineering judgment indicate that this mechanization is a logical avenue of approach for building skin friction sensors to operate over an extreme temperature range and in a vibration field. Certainly, in the absence of an obvious new approach this method must be evaluated carefully before it can be rejected.

One of the first operational systems of this generic type was used on the Aerobee-Hi missile [1]. A counter balanced flexure system was used to support the target and an LVDT (linear variable differential transformer) was used to convert flexure displacement to an electrical readout data signal. A closed loop system built by Kistler [2] is similar to the proposed system. A cooling jacket surrounds the Kistler instrument and makes operation possible from room temperature to 1500° F. The essentials of closed loop operations are: 1) skin friction force causes displacement of the flexure and displacement transducer; 2) the displacement transducer produces an electrical signal; 3) the electrical signal is amplified and used to drive a motor; 4) the motor nulls the skin friction force; 5) motor current is proportional to force and is used as the readout data signal.

It has been decided that an open loop flexure type system would be unsatisfactory because of the relatively large change in the flexure spring constant with temperature variation, the position sensors sensitivity change and sensor zero position variation with temperature. A closed loop system is sensitive to changes in the zero position of its sensor but this error can be minimized by making the flexure spring constant small. A change in the sensor zero causes a force error equal to the corresponding displacement

5

force of the flexure. Accuracy can be made almost independent of sensor sensitivity changes (theoretically it may be made completely independent in the steady state). The same is true regarding changes in the flexure spring constant and this fact is demonstrated mathematically below. As a practical matter, it appears that changes in the flexure spring constant are of little importance for a large variation in flexure temperature.

However, a closed loop system is not without disadvantages. Its accuracy depends on the servo motor force constant and it is expected that the motor force constant will vary with temperature. However, as explained in a later section, this change is reduced to only a dimensional stability problem through special motor design. The sensor sensitivity and spring constant problem of open loop type systems have been traded for a single sensitivity problem plus other advantages of closed loop operation. These advantages are: relatively small target deflection, a stiffer system and easier damping. It is believed that the sensitivity problems of the open loop system limit accuracy much more than in the case of the closed loop system but this opinion can not yet be supported without data. Having a stiffer system will reduce vibration amplitudes which, in combination with smaller deflections, will allow the separation between the engine skin and the target to be smaller than is the case for an open loop system. The main disadvantages of the closed loop approach are the necessity of adding a motor and an electronic amplifier.

It has been decided that it would be advantageous to heat the instrument electrically so that the working parts will not have to operate below some predetermined temperature. The use of a relative high minimum temperature will reduce the change in operating temperature and minimize errors due to temperature change. Depending on the final component capabilities, 200-500°F appears reasonable for the minimum operating temperature. A hermetically sealed snap action thermostat connected to a heater appears to be a practical scheme.

The best system design approach is the one which results in the smallest package volume and provides reliable operation in the specified

environment. The thickness dimension is a constraint and must not exceed 2 inches, and preferably will be less than 1-1/2 inches. It can be assumed that additional room will be available to store coolant relatively close to the skin friction meter if coolant is required. Using a coolant would simplify the design problem but would complicate the overall system. In addition, it is doubtful that enough coolant can be provided to keep the package below a destructive storage temperature after the data are obtained. It would be desirable to check calibration after the data are obtained.

The design possibility of using sufficient insulation to keep the temperature down to a tolerable level is being considered. Also, another approach is to use a combination of insulation and cooling. This combination would reduce the cooling problem and provide some protection for the package after the data are obtained.

The ideal solution from a reliability (assuming reliable high temperature components can be made) and operational point of view is to design the system so that it is capable of operating continuously in the high temperature environment. The problem of providing coolant, the possibility of damage or change in calibration due to excessive heating after the data are obtained and the possibility of malfunction due to a cooling system failure would be reduced by a design for high temperature operation. This approach is being given much consideration, but consideration is being given also to other approaches presented above because the design of a position sensor and a motor to operate in a 2000°F environment is a difficult task and may take much more time than is available, if indeed it is possible to meet the accuracy specification this way.

A block diagram of the system is contained in figure 2 and a sketch of the experimental model is contained in figure 3. The quantity F is the force input from the target and F_A is the nulling force from the servo motor.

The flexure is used only as a frictionless support. Its restoring force is not needed in the operation of the system. In fact, it is a hindrance and its effect can be neglected only if loop gain is high. To verify this, consider the response to a step input of skin friction force. The steady state output
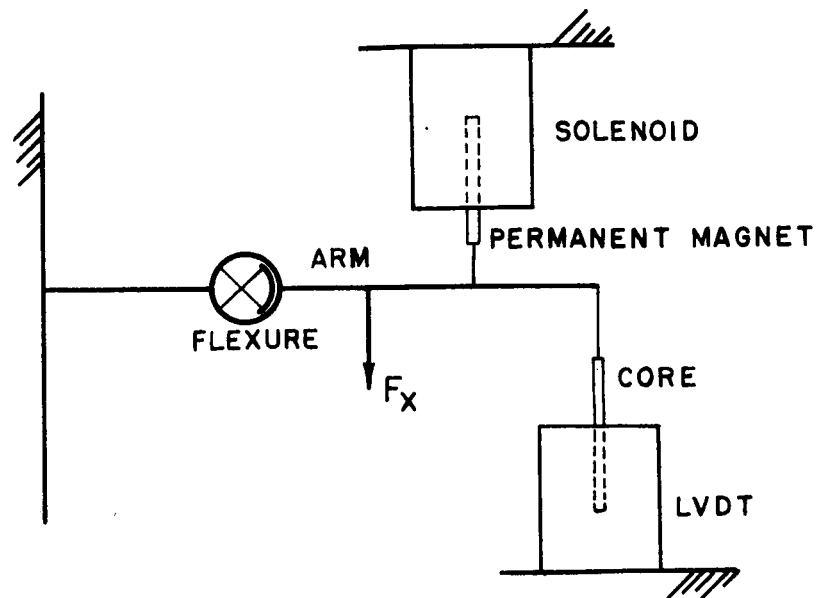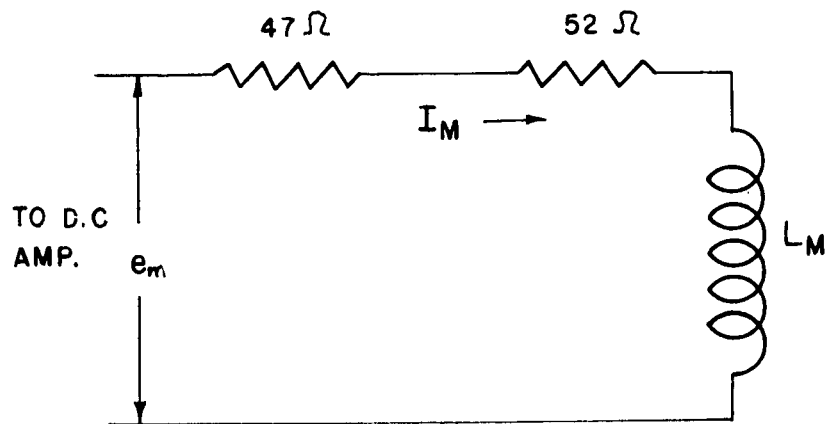
7

FIG.3   EXPERIMENTAL   MODEL

R_M = TOTAL SERIES RESISTANCE
       = 47 + 52 = 99 Ω

FIG.4   MOTOR ARMATURE EQUIVALENT
        CIRCUIT

is established analytically where:

I = total rotational inertia

B = damping due to air friction, eddy current and electrically induced damping

K_f = flexure constant; in-lbs/rad

K_t = LVDT constant; volts/mil

A = gain of dc amplifier

K_m = motor constant; grams/volt

The closed loop transfer function is:

$$\frac{C}{R}(s) = \frac{G(s)}{1 + G(s)}$$

$$= \frac{A\,K_t\,K_m}{I\,s^2 + Bs + K_f + A\,K_t\,K_m} \qquad (1)$$

For a step of force, the input is F_x/s and the steady state output is

$$C_{ss} = \lim_{s \to 0}\left\{ s\,\frac{F_x}{s}\,\frac{A\,K_t\,K_m}{I\,s^2 + Bs + K_f + A\,K_t\,K_m} \right\}$$

$$= \frac{A\,K_t\,K_m}{K_f + A\,K_t\,K_m}\,F_x \qquad (2)$$

According to Eq. 2, if $A\,K_t\,K_m \gg K_f$ then $C_{ss} = F_m \cong F_x$. Thus, feedback can make the effect of changes in K_f inconsequential.

9

The motor used in the system is a dc solenoid type with a permanent magnet field. This design allows force to be generated in forward and reverse directions although this may be of no importance. The motor is driven by a dc booster amplifier through a 47 ohm resistor. Force on the permanent magnet is directly proportional to solenoid current. The total series resistance is approximately 100 ohms. Figure 4 contains an equivalent circuit of the motor armature.

The force produced by the motor is,

$$F_m = K_m I_m \tag{3}$$

where the motor current is

$$I_m(s) = \frac{e(s)}{s L_m + R_m} . \tag{4}$$

Combining these equations yields the motor transfer function

$$\frac{F_m}{e}(s) = \frac{K_m/L_m}{s + R_m/L_m} . \tag{5}$$

The pole due to the motor, R_m/L_m is so large in frequency compared to the complex poles produced by the mass-spring system that it can be neglected. It occurs well above the cross-over frequency.

The open loop response of the system is presented in figure 5. These data were found by opening the loop at the input to the amplifier and recording the output of the LVDT. The open loop frequency response curve shows an expected resonant peak. It occurs at 5.4 Hz. With a gain of 100 the system was unstable. This is not surprising because the cross-over frequency is approximately 65 Hz based on a second order transfer function which matches the data at low frequencies. At this high a cross-over frequency, significant phase shift is probably present due to high frequency poles which have been
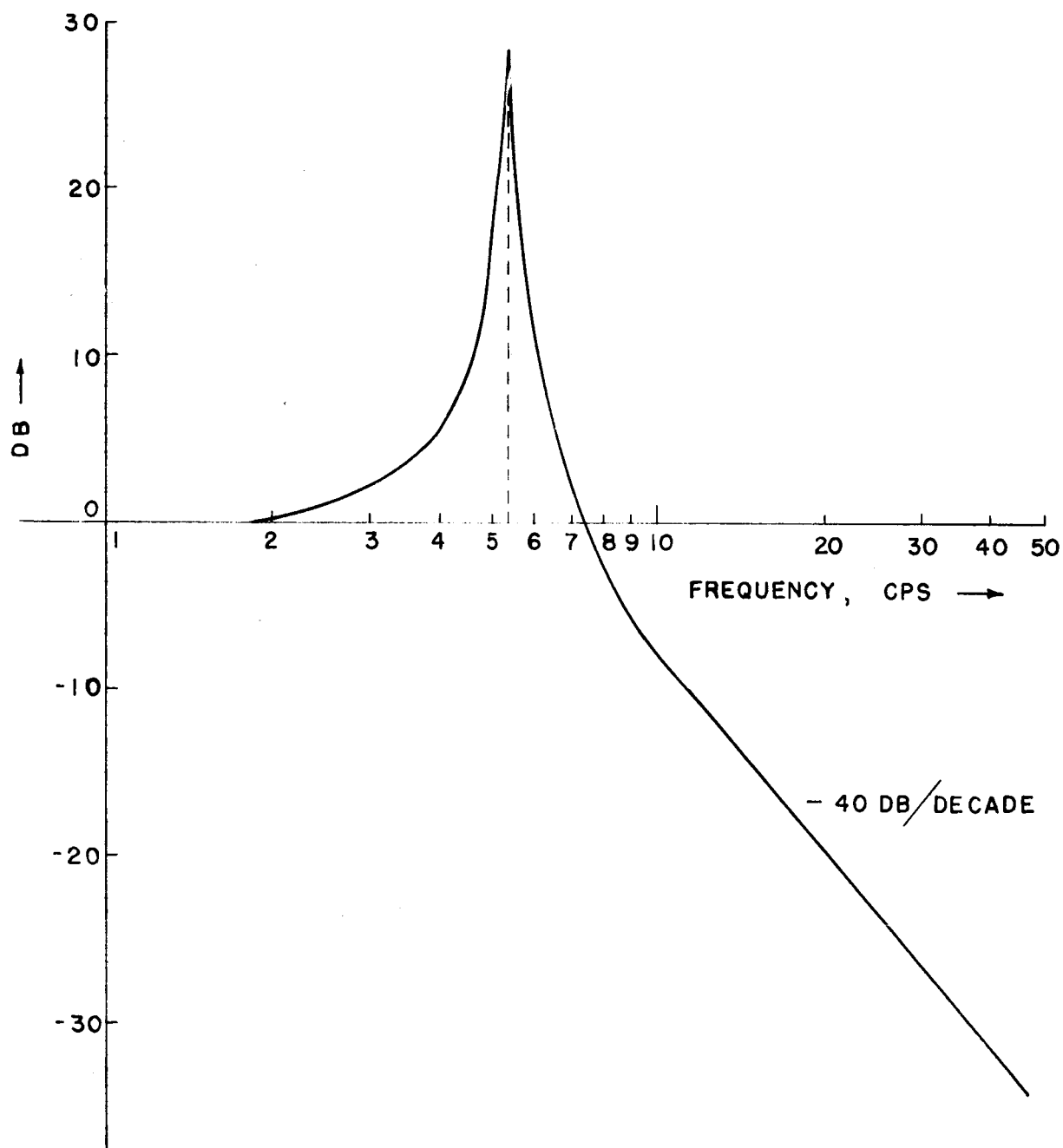
10

FIG. 5   OPEN LOOP GAIN PLOT

neglected.

In calibrating the system a known weight was applied to the pivot arm and the resulting voltage across the 47 ohm resistor was recorded. The resulting differences cannot be distinguished on the graph (figure 6). The system is very linear to the point where the amplifier saturates. The maximum force that can be measured is 4.5 gm (10 millipounds). The minimum force that can be measured has not been established.

The system constants were measured as follows:

$$\frac{K_t}{K_f} = 5.18 \text{ v/gm}$$

$$A = 100$$

$$K_m = .434 \text{ gm/v} .$$

Hence, the steady state forward gain equals

$$100 \ (5.18 \text{ v/gm})(.434 \text{ gm/v}) = 225 .$$

Hence,

$$F_m = \frac{225}{1 + 225} \ F_x = .995 \ F_x \tag{6}$$

and the measured force is 0.5% lower than the input force. This error can be removed by calibration if large variation in the open loop gain does not occur.

System particulars are:

1)   Response time: time constant = 2 seconds approximately
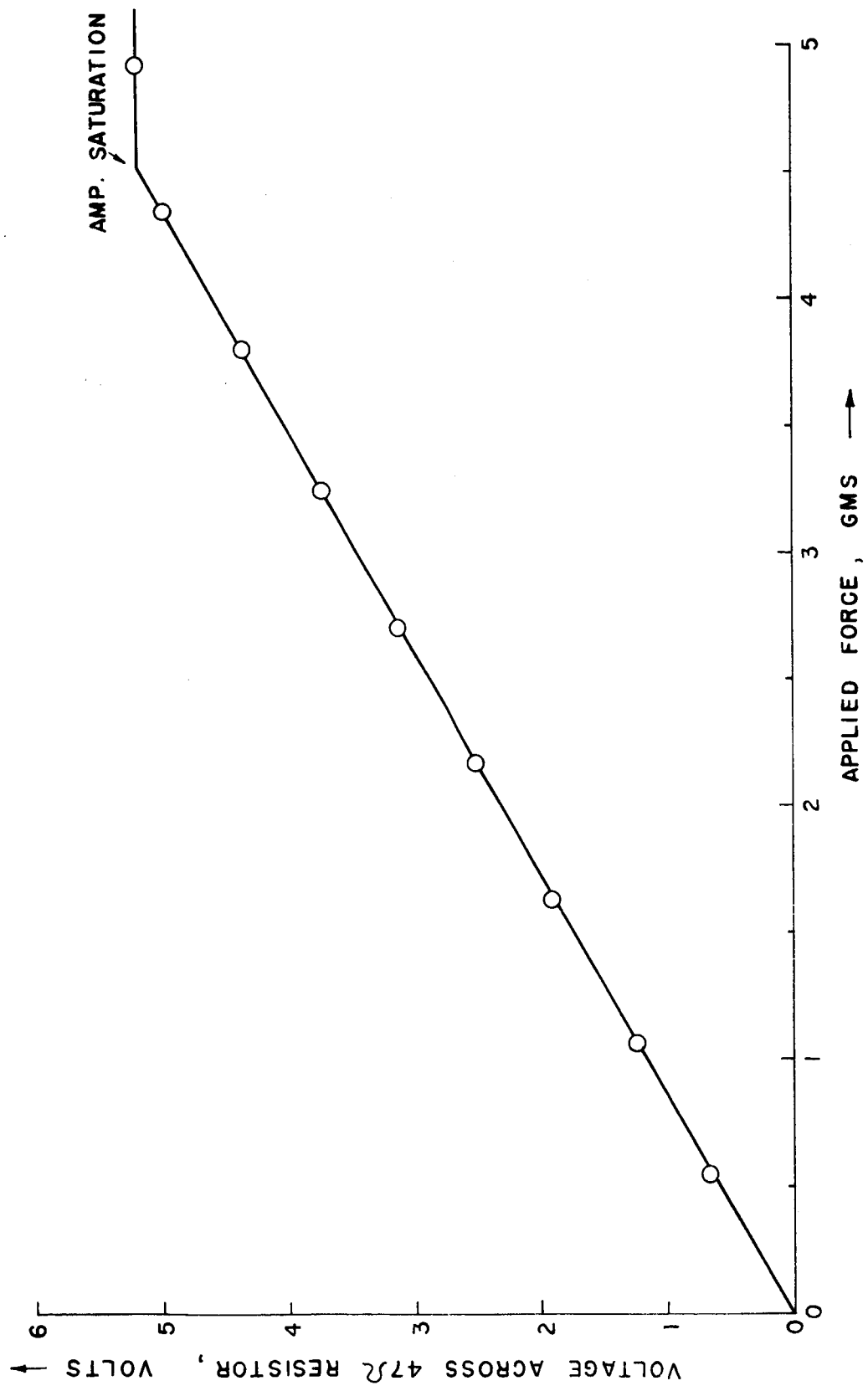2)   Natural Resonant frequency: 5.4 Hz

12

FIG. 6 SYSTEM CALIBRATION CURVE

3)   Loop gain = 225

4)   Amplifier gain = 100

5)   Maximum steady state error: 0.5 mil for 4.5 gm input

6)   Motor constant: 1.15 volts/gram

7)   Force error: -0.5% (theoretical if not removed by calibration)

The results of this investigation indicate that this type of system would be very satisfactory for force measurements when temperature and vibration effects are not considered. As high temperature components are developed they will be substituted into the system so that the temperature range can be extended. Vibration studies cannot be conducted until the mechanical parts are modified.

The response time can be made much smaller by using a different type of compensation. Response time was not considered to be important at the present, so the system was compensated in the simplest possible way.

SECTION III
DISPLACEMENT TRANSDUCERS

A.   LVDT (Linear Variable Differential Transformer)

The LVDT and capacitance bridge position transducers have advantages of simplicity, small size and possible extension to high temperature operation. These advantages make them candidates for use in the skin friction meter. In both of these transducers, relatively low frequency ac is the only input supply required. The output amplitude and phase are almost a direct (linear) function of the position of the movable part with respect to the stationary part of the device. The LVDT uses magnetic field principles and the capacitance bridge uses electric field principles. Either of the transducers will work to 2000°F in theory with suitable sensitivity. The main problem is the shift in zero displacement due to thermal effects and a choice between the transducers will probably be made on that basis.

A schematic of a conventional LVDT [3] is shown in figure 7. In principle it is nothing more than a transformer with a movable core which varies the coupling between the primary and secondary. The core is connected to the object whose position is to be sensed. Typical sensitivities are 0.1 to 1.0 volt per mil displacement and the resolution is in the neighborhood of 15 microns. Input frequencies typically range from 50-20,000 Hz. The maximum operating temperature is limited by the Curie temperature of the magnetic materials. Wire insulation too will limit operation at high temperature but magnetic material properties are the more important of the two limitations. Electrical design is relatively easy for conventional units because the magnetic fields are confined by the magnetic materials to paths of relatively low reluctance.

Thus, extension of LVDT technology appears to require two things: 1) elimination of magnetic materials; 2) development of transformer windings which will operate at high temperatures. Accuracy will depend on mechanical design and the expansion properties of the materials. An electrical schematic of the first room temperature experimental model is shown in figure 8. The iron core of low temperature designs has been replaced by a wire wound
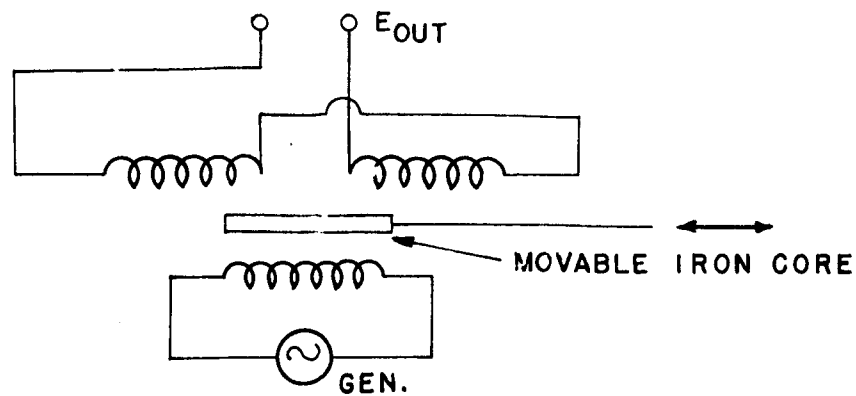
15

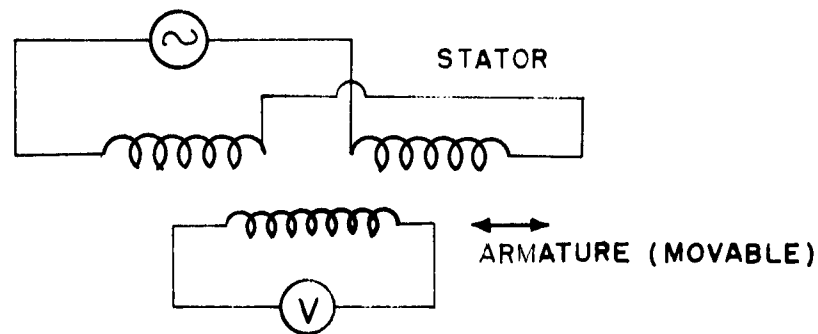FIG. 7   SCHEMATIC OF CONVENTIONAL LVDT
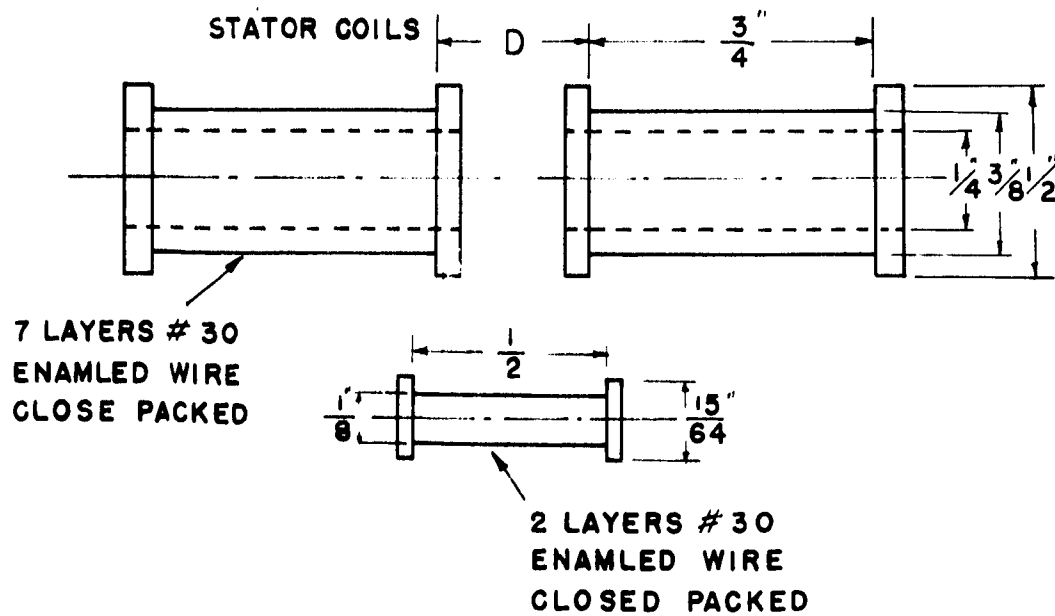

FIG. 8   SCHEMATIC OF AIR CORE LVDT

FIG. 9   PHYSICAL DIMENSIONS OF AIR CORE LVDT

16

armature. Wire and ceramic materials are being purchased to make coils which will withstand high temperatures.

The armature is concentric with both the stator coils and can move freely inside them. The stator coils are wound so they produce fluxes in opposite directions. Thus, when the center of the armature is exactly half way between the stator coils it will have equal but opposite voltages induced in it and the resultant emf across its terminals should be zero. Any movement to the left or right will cause an unbalance of flux linkages and a new induced voltage greater than zero. The phase of the induced voltage depends on the direction of movement from the null position. Specifications for the LVDT tested are shown in figure 9.

Data were taken relating voltage induced in the armature to displacement from null position for figure 10, relating null voltages to coil separation d, figure 11. In these measurements the input frequency was 10 KHz, and the stator coil voltage was held constant at 0.5 volt rms. A few measurements were taken with the armature and field functions reviewed in case this information might be useful, i.e., the armature was the energized winding. No appreciable difference was noted in these data from those of figure 10.

Curves of voltage versus displacement (stroke) were plotted for stator coil separations of 5/8" and 7/8". It is seen that as the coil separation is decreased the null voltage increased but the slope about null is greater. The null voltage is not zero because the stator coil geometries are not identical, although they ideally would be, and capacitance effects are introduced which cause the null voltage. With careful design and construction it is believed that a near zero null can be achieved. As the coil separation is increased beyond 3/4" the null voltage decreases very slowly and dead band begins to appear. The sensitivity at large coil separation is very low. At small coil separations the sensitivity is much higher but a good null is more difficult to achieve. Somewhere between these two extremes is an optimum spacing. The optimum spacing appears to be in the neighborhood of 0.6 to 0.7 inches.

An excitation frequency of 100 KHz was tried but very little voltage was induced into the armature because impedance levels increased and
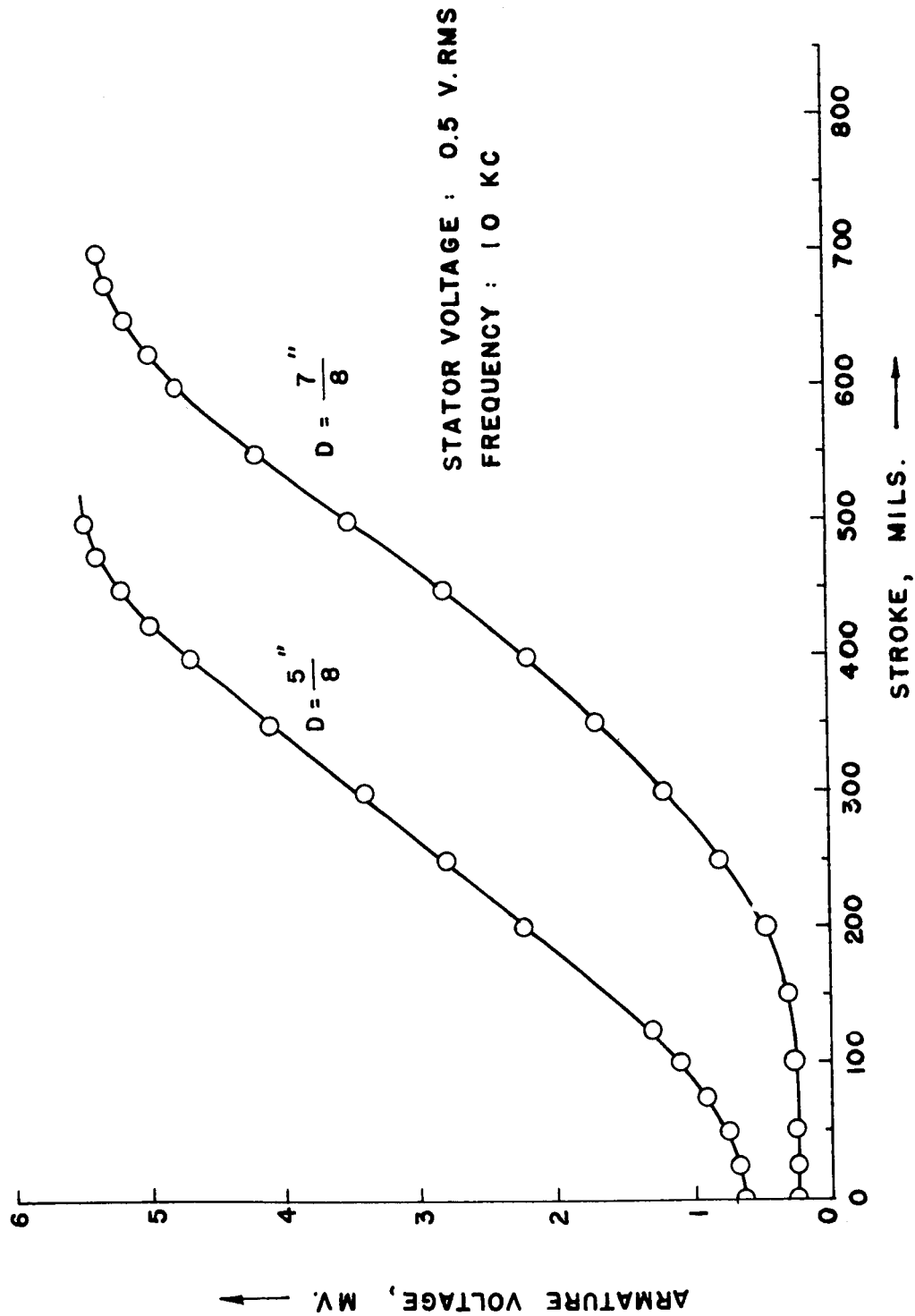
17

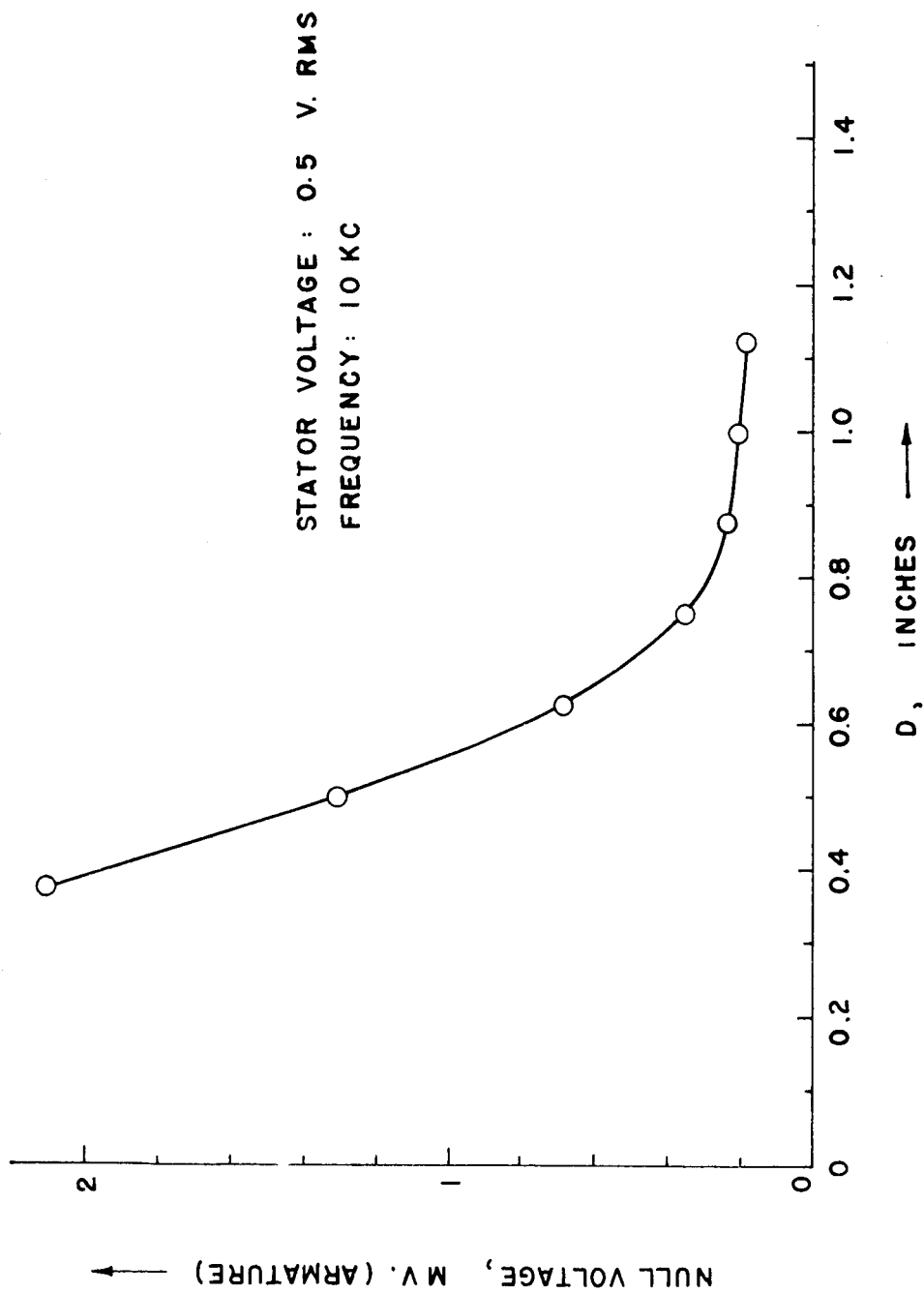FIG. 10   INDUCED VOLTAGE VERSUS DISPLACEMENT
FOR AIR CORE LVDT

STATOR VOLTAGE : 0.5 V. RMS
FREQUENCY : 10 KC

D, INCHES ——→

NULL VOLTAGE, M V. (ARMATURE) ——→

FIG. 11 NULL VOLTAGE VERSUS STATOR COIL
SEPARATION D.

19

reduced the excitation current.

B.   Capacitance Bridge

A capacitance type transducer does not have difficult insulation problems of the type present in the LVDT at high temperatures. The basic construction is with plates instead of wires. This may yield a basic advantage in regard to zero position drift. An electrical schematic of the bridge is shown in figure 12 and a sketch of a model being constructed is shown in figure 13.

The four fixed plates are the same size and positioned so that no stray capacitance exists between the movable plate and the fixed plates of C, not common to C_2 and C_3. (A sufficiently large gap between the fixed plates will insure this.) No wire need be run to the movable plate since it can be made to have ground potential. From figure 12 note that

$$e_0 = \left(\frac{j\omega C_1}{j\omega C_1 + j\omega C_1} - \frac{j\omega C_2}{j\omega C_2 + j\omega C_3} \right) E$$

$$= \frac{C_3 - C_2}{C_3 + C_2} \frac{E}{2} . \tag{7}$$

At the null position $C_2 = C_3$ and $e_0 = 0$. Suppose the movable plate is displaced from null so that C_3 is increased by increasing the area of capaciter C_3. Then, C_2 is decreased by the same amount and

$$\Delta e_0 = \frac{(C_2 + \Delta C) - (C_2 - \Delta C)}{C_2 + \Delta C + C_2 - \Delta C} \frac{E}{2}$$

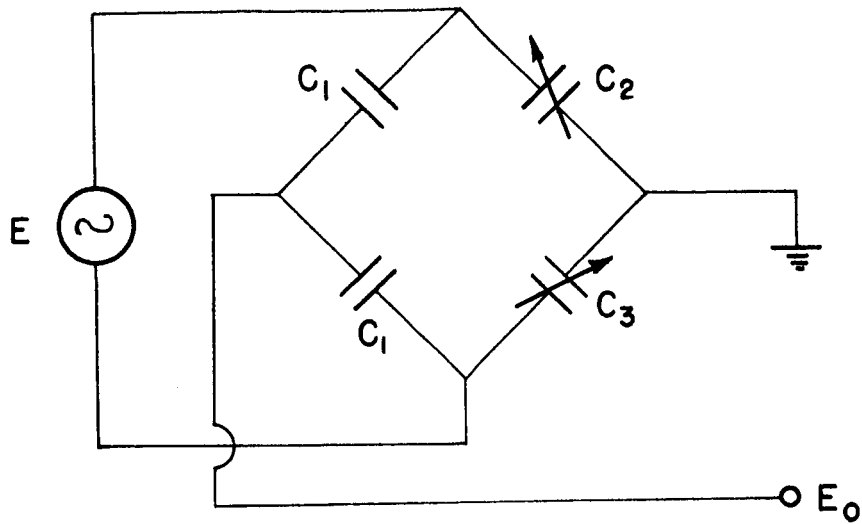$$= \frac{\Delta C}{C_2} \frac{E}{2} . \tag{8}$$

FIG. 12   SCHEMATIC OF CAPACITIVE TRANSDUCER
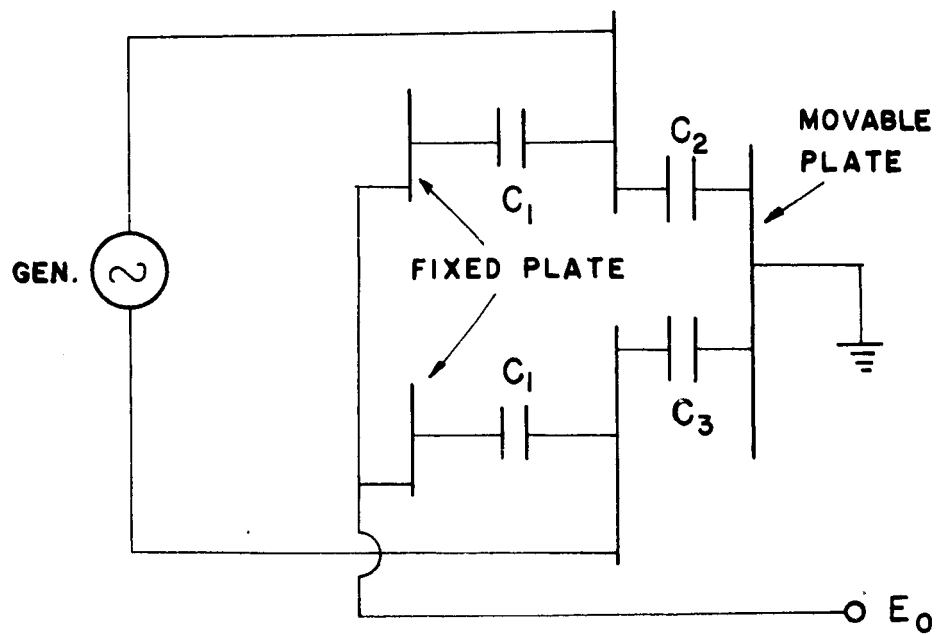
FIG. 13   CONSTRUCTION OF CAPACITIVE
TRANSDUCER

At null, $C_2 = C_3 = C_1$ and the output impedance of the bridge is $1/4\, j\omega\, C_1$.

The size of the capacitors required and the operating frequency depend on the maximum allowable output impedance. If an amplifier having an input impedance of 1 meg-ohm or greater is used, the bridge output impedance can be 50 K or lower without causing significant loading effects. Assume f = 100 KHz, for example. Then

$$\frac{1}{2\pi f C_1} = 4 \times 50,000$$

and

$$C_1 = \frac{1}{6.28 \times 2 \times 10^5 \times 10^5} = \frac{100}{12.56} \times 10^{-12}$$

$$= 8 \text{ pf.} \tag{9}$$

It can be shown that

$$C_1 = \frac{\epsilon A}{d} .$$

Let:

   d (plate separation) = 20 mils

and ϵ = permitivity of air.

Solving for A yields:

$$A = \frac{8 \times 10^{-12} \times 5.08 \times 10^{-4}}{8.85 \times 10^{-12}} = 4.6 \times 10^{-4} \text{m}^2 = 0.72 \text{ in}^2 .$$

$$\tag{10}$$

The plates could have dimensions such as 1" × 0.72".

Let E = 50 volts. If the movable plate is displaced 1 mil from null position,

$$\frac{\Delta C}{C} = \frac{0.001}{0.72} \tag{11}$$

and

$$\Delta e_0 = \frac{1}{720} \quad \frac{50}{2} = 33.4 \text{ mv} . \tag{12}$$

A relatively low gain would be needed to produce an output capable of driving a motor with the calculated sensitivity.

The size of the plates may be reduced in various ways. Plate spacing d may be reduced, the operating frequency may be raised or the output impedance increased. The first method results in a smaller area required to produce a given capacitance and the latter two result in a smaller required capacitance. Additional investigation will establish the best approach to be followed.

Varying capacitance by changing area seems perferrable to changing spacing because expansion effects can be more easily compensated. It is believed that expansion will change spacing equally among the plates and changes in area due to elongation or contraction can be controlled so that even though C changes the null position will remain unchanged.

SECTION IV
MOTOR DESIGN

The room temperature experimental model used a dc motor consisting of a solenoid with a permanent magnet (Alnico 5) armature. A solenoid is 1-1/2 inches long and has 16 layers of #30 magnet wire random wound. This together with a 1/8" diameter magnet gave a force of approximately 10 millipounds for a solenoid current of 100 ma (the limit of the Philbrick booster amplifier used). The permanent magnet armature has two distinct advantages (as compared to a coil of wire for the armature): 1) wires do not have to be placed on moving parts; 2) relatively high flux density is easy to obtain. These advantages are not possible at temperatures above the Curie temperature. Thus, the armature field will have to be obtain from a current coil in a system which will work in a 2000°F environment.

Two approaches for the development of a high temperature actuator have been studied. These are the capacitor motor and the solenoid motor with no magnetic materials. The solenoid seems ideal for use in a high temperature environment because force is nearly independent of displacement over a large displacement range. Thus, relatively large changes in position between the solenoid and armature due to thermal expansion and target displacement will have little effect on armature force. However, when one considers the dimensions of the motor used in the experimental model there seems to be little hope of designing a solenoid motor small enough to do the job. Calculations support this opinion, so a different configuration must be considered.

A capacitor motor would consist of two plates with small separation. One plate is fixed (stator) and one is movable. It can be shown that the force on the movable plate is

$$F = \frac{E^2 \epsilon A}{2 d^2} \tag{13}$$

where:

        E   =   voltage across the plates

        ϵ =   permitivity of separating material

        A   =   area of each plate

        d   =   plate separation

To get an indication of the size of the forces present, some numbers were assumed. It was assumed that in keeping with the dimensions of the unit the plates would be 1/2" square (A = 1/4 sq. in.), and that E would be 50 volts. For an F of 10 millipounds d is .25 milli-inch. This calculation brings to light two problems: 1) because of the small separation required, expansion affects would play a dominant role; from the equation for force it is seen that force varies inversely as the square of displacement; 2) the small separation might cause arcing in the high altitude high temperature environment. The latter problem could be overcome by placing a dialetric between the plates. This would increase ϵ and result in a larger d needed to give the maximum force, a disadvantage. However, the behavior of a dialetric at such high temperatures is uncertain and may not be practical. The nonlinearity of the motor force constant as a function of d is a calibration problem too. A displacement of d = 10 mils would be required to make the motor force constant relatively independent of zero position drift. A 10 mil displacement appears to make the motor impractical.

At this point it appears that a motor employing magnetic effects is the best approach but that a physical configuration other than a solenoid is necessary. New configurations are being considered.

26

SECTION V
ELECTRONIC PACKAGE

The minimum electronics required will be an amplifier to amplify the displacement transducers output to a level which will drive the motor. In its simplest form this would be an ac amplifier with a gain of approximately 100. An ac motor would be required in this case and the amplifier would contain two or three stages. An ac system eliminates the need for a demodulator and dc amplifiers. DC amplifiers are more difficult to build than ac amplifiers.

There is little hope of building an electronic amplifier which will operate in a 2000°F ambient. It is more likely that a displacement transducer could be built with sufficient power handling ability than that an electronic amplifier could be built which will not have to be cooled. Two obvious approaches to the problem are to either place the amplifier in the aircraft or imbed it in insulation and place it in a remote location with respect to the skin friction measurement package. With silicon transistors the inside package temperature may reach a maximum permissible temperature in the neighborhood of 175°C. The self heating of the amplifier package may be a significant part of the total problem. This problem is being studied and a definite answer will be available soon on the practicability of this problem. If necessary, a crude cooling system will be designed.

The amplifier need not be nondestructive. It merely has to operate during the data gathering period. If the gain is greater than a minimum value the calibration will be essentially independent of gain. This means that the calibration may be obtained after the test by inserting a new amplifier into the system. That the test results are independent of amplifier gain can be seen by noting:

$$F_m(\text{steady state}) = \frac{A\,K_T K_m}{K_F + AK_T K_m}\,F_x \qquad (14)$$

27

where

$$K_m = .434 \frac{gm}{volt} \quad , \quad \text{for the system tested}$$

$$\frac{KT}{KF} = 5.18 \frac{v}{gm} \quad .$$

Suppose the force error is to be less than 1%. Then,

$$\frac{\dfrac{A \, K_T \, K_m}{K_f}}{1 + \dfrac{A \, K_T K_m}{K_F}} > 0.99 \tag{15}$$

or

$$\frac{2.25 \, A}{1 + 2.25 \, A} > 0.99 \quad . \tag{16}$$

From this is apparent that $A > 44$. Thus if A is made greater than 44 calibration will be relatively independent of amplifier gain variations.

SECTION VI

PNEUMATIC CONTROL SYSTEM

A pneumatic control system offers the best chance of meeting the temperature specifications. Several possible configurations could be devised but a workable one would be to have the same block diagram as that for the electronic control system, figure 2, except the electronic components would be replaced by pneumatic components. Thus the same gains would yield a system having the same static accuracy, the same maximum displacement, and approximately the same physical configuration. Pneumatic systems are generally limited in maximum temperature only by the materials of which they are made. Another advantage is their relative insensitivity to vibration and shock. Their major disadvantages in this application is the continuous loss of pneumatic media and possibly in their slower response times. It is expected, however, that response times will be considerably faster than the inertia portions of the system and thus should be adequate.

A schematic diagram of a pneumatic control system is shown in figure 14. The system is the counter balanced moving arm system for the breadboard model shown in figure 3. The force to be measured enters the system as a load disturbance. A pneumatic sensor, amplifier, and motor are required with the amplifier section including compensation if necessary. The position sensor uses two gas jets connected to a pressure supply so that it acts as a Wheatstone bridge. Orifice size is on the order of 5 to 10 mils and control gap is on the order of 1 mil. Thus air flow is small. Displacement of the sensor vane creates a differential pressure ΔP in the plenum. This ΔP controls the jet of a proportional amplifier which then feeds additional amplifier stages leading eventually to a back-to-back set of pneumatic pressure motors. Actually the entire control system acts as a back-to-back system. This will tend to give sharpness to the response to small disturbances.

The motors in this system are quite similar to a pair of variable pressure air bearings. However their volumn is large compared to an air bearing and thus their equivalent dynamic spring constant is low. Their
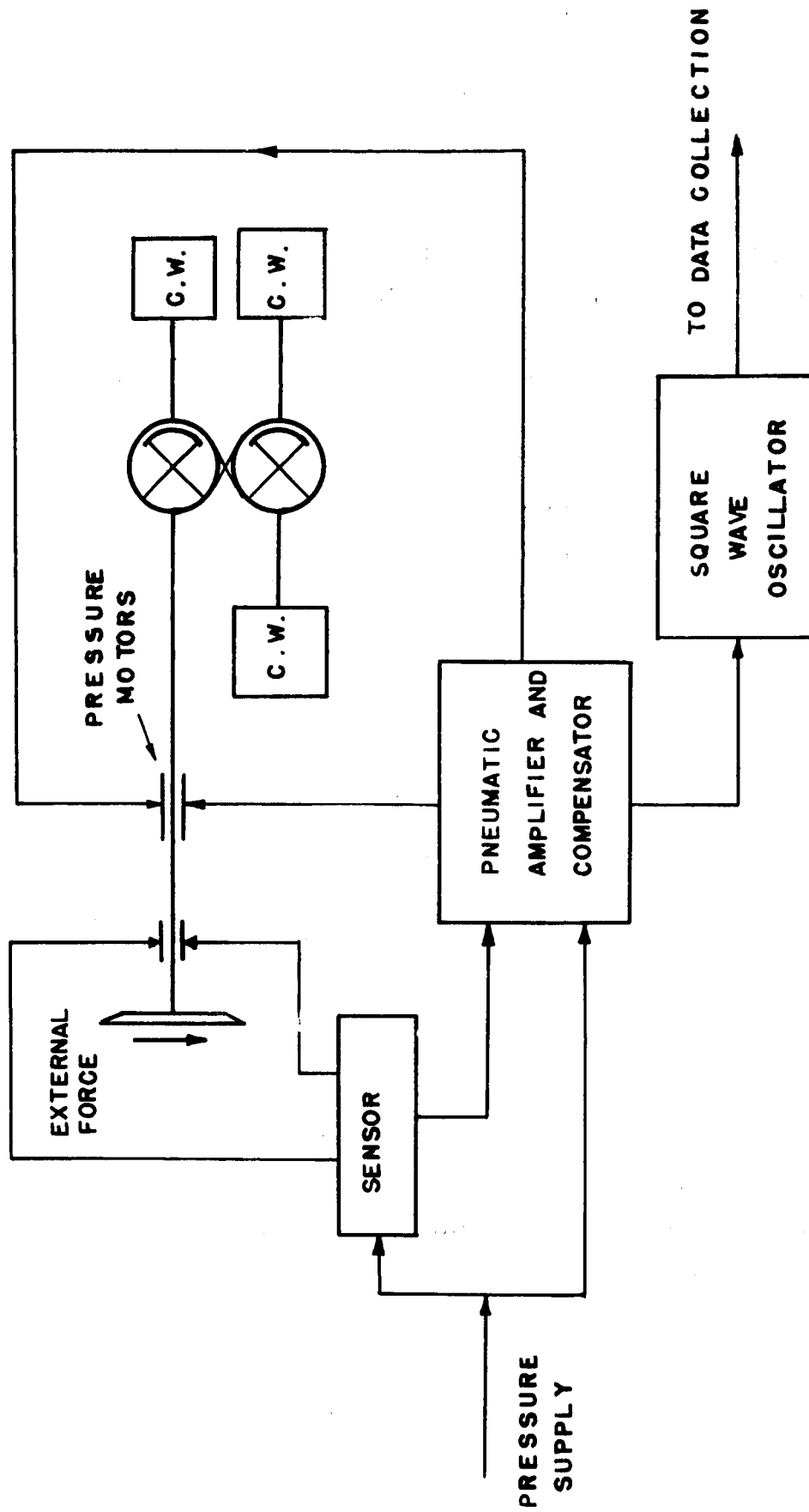
29

FIG. 14   PNEUMATIC SYSTEM

actual spring constant will depend on the open loop gain of the system.

The equations of motion of the system are:

$$J\ddot{\theta} + K_1\theta = F_m r_2 + Dr_1$$

where

θ = angular displacement

J = polar moment of inertia

F_m = motor force

r_2 = motor moment arm

D = drag force

r_1 = test section moment arm.

From the electrical section the required static gain varies from 100 to 225: taking the larger figure, the static gain of the fluid system is

$$Gain = 800\,K\,A\,r_2\,r_1 = 225$$

where 800 is a typical gain for a pneumatic sensor. Assuming a motor diameter of .25-in., A is .049-sq.in. The moment arm r_1 is 1" and r_2 is .5-in. Thus $K = 11.5$ is the required gain of the pneumatic amplifier. This is equivalent to two stages of a Corning load sensitive fluid amplifier or to three stages of a load insensitive amplifier.

To·gain full advantage of the fluidic system it will be necessary to use fluids all the way back to the data collection point. It will be advantageous to convert some signal, say motor differential pressure, into a square wave signal by using it to run a pressure sensitive oscillator. The frequency of the signal will then be proportional to the skin friction drag.

This approach is only in the preliminary design stage since the major effort, after the initial study period, has been in design and development of the electrical system.

31

SECTION VII
MULTICOMPONENT MICROFORCE
BALANCE SYSTEM

The prototype system construction is complete and final calibration data are being obtained. It appears that all original research goals are being met. The prototype will be shipped to NASA Langley Field by the end of February, it is anticipated. Final reports will be available by early spring. At least one more paper will be written on this system. The first paper has been accepted and will be presented at the International Federation of Automatic Control Conference at London, England in June 1966.

Two more masters theses will be completed on this system by June, 1966.

SECTION VIII
CONCLUSIONS

The only skin friction sensor which can be built within the grant period which ends June 15, 1966 is an insulated and cooled model using low temperature components. The minimal operating temperature will be established using a snap action thermostat and an electrical heater. Work is presently in progress on a prototype model. Experimental electrical components have been built.

The state-of-the art in motor and sensor design for high temperature operation is being extended by making components which will operate in a 2000°F environment. Experimental models of a sensor and motor are now being built. The remaining problem in the high temperature system is the development of high temperature flexure pivots. It appears that this will be feasible using possibly beryllium or Hastelloy components throughout. As soon as materials are received experimentation will start on high temperature flexures to be used with the high temperature sensor and motor which is already under development.

The study of a completely pneumatic system is also proceeding, although very slowly. There may be time and funds to build a breadboard model but the major effort is expected to continue to be on the electronic system.

REFERENCES

1. F. W. Fenter and W. C. Lyons, Jr., "The Direct Measurement of Local Skin Friction or Aerobee-Hi Rockets in Free Flight," DRL-391, CM-877, Defense Research Laboratory, The University of Texas, Texas; May 1957.

2. "Kistler Skin Friction Drag Sensor," Files of Force Measurements Group, Instrument Research Division, NASA, Langley Field, Virginia.

3. Lion, Instrumentation in Scientific Research, p. 48, McGraw-Hill; 1959.

36